

A statistical view on a surrogate model for estimating extreme events with an application to wind turbines

Mikkel Slot Nielsen and Victor Rohde

Department of Mathematics, Aarhus University,
 {mikkel, victor}@math.au.dk

Abstract

In the present paper we propose a surrogate model, which particularly aims at estimating extreme events from a vector of covariates and a suitable simulation environment. The first part introduces the model rigorously and discusses the flexibility of each of its components by drawing relations to literature within fields such as incomplete data, statistical matching, outlier detection and conditional probability estimation. In the second part of the paper we study the performance of the model in the estimation of extreme loads on an operating wind turbine from its operational statistics.

AMS 2010 subject classifications: 62P30; 65C20; 91B68

Keywords: extreme event estimation; wind turbines; surrogate model

1 Introduction

Suppose that we want to assess the distributional properties of a certain one-dimensional random variable Y . For instance, one could be interested in knowing the probability of the occurrence of large values of Y as they may be associated with a large risk such as system failure or a company default. One way to evaluate such risks would be to collect observations y_1, \dots, y_n of Y and then fit a suitable distribution (e.g., the generalized Pareto distribution) to the largest of them. Extreme event estimation is a huge area and there exists a vast amount on literature of both methodology and applications; a few references are [4, 5, 12, 17]. This is one example where knowledge of the empirical distribution of Y ,

$$\widehat{\mathbb{P}}_Y(\delta_{y_1}, \dots, \delta_{y_n}) = \frac{1}{n} \sum_{i=1}^n \delta_{y_i}, \quad (1.1)$$

is valuable. (Here δ_y denotes the Dirac measure at the point y .) If one is interested in the entire distribution of Y , one may use the estimator (1.1) directly or a smoothed version, e.g., replacing δ_{y_i} by the Gaussian distribution with mean y_i and variance $\sigma^2 > 0$ (the latter usually referred to as the bandwidth). The problem in determining (1.1) arises if Y is not observable. Such a situation can happen for several reasons, e.g., it may be that Y is difficult or expensive to measure or that its importance has just recently been recognized, and hence one have not collected the historic data that is needed. Sometimes, a solution to the problem of having a latent variable could be to set up a suitable simulation environment and, by varying the conditions of the system, obtain various realizations of Y . Since we cannot be sure that the variations in the simulation environment correspond to the variations in the physical environment, the realizations of Y are not necessarily drawn from the true distribution. This is essentially similar to any experimental study and one will have to rely on the existence of control variables.

By assuming the existence of an observable d -dimensional vector X of covariates carrying information about the environment, a typical way to proceed would be regression/matching which in turn would form a surrogate model. To be concrete, given a realization x of X , a surrogate model is expected to output (approximately) $f(x) = \mathbb{E}[Y \mid X = x]$, the conditional mean of Y given $X = x$. Consequently, given inputs x_1, \dots, x_n , the model would produce $f(x_1), \dots, f(x_n)$ as stand-ins for the missing values y_1, \dots, y_n of Y . Building a surrogate for the distribution of Y on top of this could now be done by replacing y_i by $f(x_i)$ in (1.1) to obtain an estimate $\widehat{\mathbb{P}}_Y(\delta_{f(x_1)}, \dots, \delta_{f(x_n)})$ of the distribution of Y . This surrogate model for the distribution of Y can thus be seen as a composition of two maps:

$$(x_1, \dots, x_n) \longrightarrow (\delta_{f(x_1)}, \dots, \delta_{f(x_n)}) \longrightarrow \widehat{\mathbb{P}}_Y(\delta_{f(x_1)}, \dots, \delta_{f(x_n)}). \quad (1.2)$$

In the context of an incomplete data problem, the strategy of replacing unobserved quantities by the corresponding conditional means is called regression imputation and will generally not provide a good estimate of the distribution of Y . For instance, while the (unobtainable) estimate in (1.1) converges weakly to the distribution of Y as the sample size n increases, the one provided by (1.2) converges weakly to the distribution of the conditional expectation $\mathbb{E}[Y \mid X]$ of Y given X . In fact, any of the so-called single imputation approaches, including regression imputation, usually results in proxies $\hat{y}_1, \dots, \hat{y}_n$ which exhibit less variance than the original values y_1, \dots, y_n , and in this case $\widehat{\mathbb{P}}_Y(\delta_{\hat{y}_1}, \dots, \delta_{\hat{y}_n})$ will provide a poor estimate of the distribution of Y (see [15] for details).

The reason that the approach (1.2) works unsatisfactory is that $\delta_{f(x)}$ is an (unbiased) estimator for the distribution of $\mathbb{E}[Y \mid X]$ rather than of Y . For this reason we will replace $\delta_{f(x)}$ by an estimator for the conditional distribution μ_x of Y given $X = x$ and maintain the overall structure of (1.2):

$$(x_1, \dots, x_n) \longrightarrow (\mu_{x_1}, \dots, \mu_{x_n}) \longrightarrow \widehat{\mathbb{P}}_Y(\mu_{x_1}, \dots, \mu_{x_n}). \quad (1.3)$$

In Section 2 we introduce the model (1.3) rigorously and relate the assumptions on the simulation environment needed to estimate μ_x to the classical strong ignorability (or unconfoundedness) assumption within a matching framework. Given a simulation environment that satisfies this assumption, an important step in order to apply the surrogate model (1.3) is of course to decide how to estimate μ_x , and hence we discuss in Section 2.1 some methods that are suitable for conditional probability estimation. In Section 2.2 we address the issue of checking if the simulation environment meets the imposed assumptions. Finally, in Section 3 we apply the surrogate model to real-world data as we estimate extreme tower loads on a wind turbine from its operational statistics.

2 The model

Let \mathbb{P} be the physical probability measure. Recall that Y is the one-dimensional random variable of interest, X is a d -dimensional vector of covariates and x_1, \dots, x_n are realizations of X under \mathbb{P} . We are interested in a surrogate model that delivers an estimate of $\mathbb{P}(Y \in B)$ for every measurable set B . The model is given by

$$\widehat{\mathbb{P}}_Y = \frac{1}{n} \sum_{i=1}^n \widehat{\mu}_{x_i}, \quad (2.1)$$

where $\widehat{\mu}_x$ is an estimator for the conditional distribution μ_x of Y given $X = x$. Since each x_i is drawn independently of μ_x under \mathbb{P} , each $\widehat{\mu}_{x_i}$ provides an estimator of \mathbb{P}_Y , and the averaging in (2.1) may be expected to force the variance of the estimator $\widehat{\mathbb{P}}_Y$ to zero as n tends to infinity. In order to obtain $\widehat{\mu}_x$ we need to assume the existence of a valid simulation tool:

Condition 2.1. Realizations of (X, Y) can be obtained under an artificial probability measure \mathbb{Q} which satisfies

- (i) The support of $\mathbb{P}(X \in \cdot)$ is contained in the support of $\mathbb{Q}(X \in \cdot)$.
- (ii) The conditional distribution of Y given $X = x$ is the same under both \mathbb{P} and \mathbb{Q} , that is,

$$\mathbb{Q}(Y \in \cdot \mid X = x) = \mu_x$$

for all x in the support of $\mathbb{P}(X \in \cdot)$.

In words, Condition 2.1 says that any outcome of X that can happen in the real world can also happen in the simulation environment and, given an outcome of X , the probabilistic structure of Y in the real world is perfectly mimicked by the simulation tool. Note that, while this is a rather strict assumption, it may of course be relaxed to $\mathbb{Q}(Y \in B \mid X = x) = \mu_x(B)$ for all x in the support of $\mathbb{P}(X \in \cdot)$ and any set B of interest. For instance, in Section 3 we will primarily be interested in $B = (\tau, \infty)$ for a large threshold τ .

Remark 2.2. We can assume, possibly by modifying the sample space, the existence of a random variable $Z \in \{0, 1\}$ and a probability measure $\tilde{\mathbb{P}}$ such that

$$\mathbb{P} = \tilde{\mathbb{P}}(\cdot \mid Z = 0) \quad \text{and} \quad \mathbb{Q} = \tilde{\mathbb{P}}(\cdot \mid Z = 1).$$

Effectively, Z indicates whether we are using the simulation tool or not, and $\tilde{\mathbb{P}}(Z = 1) \in (0, 1)$ defines the probability of drawing (X, Y) from the simulation environment (as opposed to drawing X from the measurement environment). In this case, according to Bayes' rule, Condition 2.1 is equivalent to

$$\tilde{\mathbb{P}}(Z = 1 \mid X, Y) = \tilde{\mathbb{P}}(Z = 1 \mid X). \quad (2.2)$$

In words, (2.2) means that Y and Z are conditionally independent under $\tilde{\mathbb{P}}$ given X . The assumption (2.2) was introduced in Rosenbaum and Rubin [13] as the strong ignorability assumption in relation to estimating heterogeneous treatment effects. In the literature on incomplete data, where Z indicates whether Y is observed or not, (2.2) is usually known as the Missing at Random (in short, MAR) mechanism, referring to the pattern of which Y is missing. This assumption is often imposed and viewed as necessary in order to do inference. See [9, 14, 15] for details about the incomplete data problem and the MAR mechanism.

Remark 2.3. Usually, to meet Condition 2.1(ii), one will search for a high-dimensional X (large d) to control for as many factors as possible. However, as this complicates the estimation of μ_x , one may be interested in finding a function $b : \mathbb{R}^d \rightarrow \mathbb{R}^m$, $m < d$, maintaining the property

$$\mathbb{P}(Y \in \cdot \mid b(X) = b(x)) = \mathbb{Q}(Y \in \cdot \mid b(X) = b(x)) \quad (2.3)$$

for all x in the support of $\mathbb{P}(X \in \cdot)$. This is a well-studied problem in statistical matching with the main reference being Rosenbaum and Rubin [13], who referred to any such b as a balancing function. They characterized the class of balancing functions by first showing that (2.3) holds if b is chosen to be the propensity score under $\tilde{\mathbb{P}}$ (cf. Remark 2.2), $\pi(x) = \tilde{\mathbb{P}}(Z = 1 \mid X = x)$, and next arguing that a general function b is a balancing function if and only if

$$f(b(x)) = \pi(x) \quad \text{for some function } f. \quad (2.4)$$

2.1 Estimation of the conditional probability

The ultimate goal is to estimate $\mu_x = \mathbb{Q}(Y \in \cdot \mid X = x)$, e.g., in terms of the cumulative distribution function (CDF) or density function, from a sample $(x_1^s, y_1^s), \dots, (x_m^s, y_m^s)$ of (X, Y) under the artificial measure \mathbb{Q} . (We use the notation x_i^s rather than x_i to emphasize that the quantities are simulated values and should not be confused with x_i in (2.1).) The literature on conditional probability estimation is fairly large and includes both parametric and non-parametric approaches

varying from simple nearest neighbors matching to sophisticated deep learning techniques. A few references are [7, 8, 10, 18]. In Section 3 we have chosen to use two simple but robust techniques in order to estimate μ_x :

- (i) *Smoothed k -nearest neighbors*: for a given $k \in \mathbb{N}$, $k \leq m$, let $I_k(x) \subseteq \{1, \dots, m\}$ denote the k indices corresponding to the k points in $\{x_1^s, \dots, x_m^s\}$ which are closest to x with respect to some distance measure. Then μ_x is estimated by

$$\hat{\mu}_x = \frac{1}{k} \sum_{i \in I_k(x)} \mathcal{N}(y_i^s, \sigma),$$

where $\mathcal{N}(\xi, \sigma)$ denotes the Gaussian distribution with mean ξ and standard deviation $\sigma \geq 0$ (using the convention $\mathcal{N}(\xi, 0) = \delta_\xi$).

- (ii) *Smoothed random forest classification*: suppose that one is interested in the CDF of μ_x at certain points $\alpha_1 < \alpha_2 < \dots < \alpha_k$ and consider the random variable $C \in \{0, 1, \dots, k\}$ defined by $C = \sum_{j=1}^k \mathbb{1}_{\{Y > \alpha_j\}}$. From y_1^s, \dots, y_m^s one obtains realizations c_1, \dots, c_m of C under \mathbb{Q} and, next, random forest classification (as described in [2]) can be used to obtain estimates of the functions

$$p_j(x) = \mathbb{Q}(C = j \mid X = x), \quad j = 0, 1, \dots, k-1.$$

Given these estimates, say $\widehat{p}_0, \widehat{p}_1, \dots, \widehat{p}_{k-1}$, the CDF of μ_x is estimated by

$$\widehat{\mu}_x((-\infty, \alpha_i]) = \sum_{j=1}^k \widehat{p}_{j-1}(x) \Phi\left(\frac{\alpha_i - \alpha_j}{\sigma}\right), \quad i = 1, \dots, k,$$

where Φ is the CDF of a standard Gaussian distribution (using the convention $\Phi(\cdot/0) = \mathbb{1}_{[0, \infty)}$).

Both techniques are easily implemented in Python using modules from the scikit-learn library (see [11]). The distance measure d , referred to in (i), would usually be of the form

$$d(x, y) = \sqrt{(x - y)^T M (x - y)}, \quad x, y \in \mathbb{R}^d,$$

for some positive definite $d \times d$ matrix M . If M is the identity matrix, d is the Euclidean distance, and if M is the inverse sample covariance matrix of the covariates, d is the Mahalanobis distance. Note that, since the k -nearest neighbors (k NN) approach suffers from the curse of dimensionality, one would either require that X is low-dimensional, reduce the dimension by applying dimensionality reduction techniques or use another balancing function than the identity function (i.e., finding an alternative function b satisfying (2.4)).

2.2 Validation of the simulation environment

The validation of the simulation environment concerns how to evaluate whether or not Condition 2.1 is satisfied. Part (i) of the condition boils down to checking whether it is plausible that a realization x of X under the physical measure \mathbb{P} could also happen under the artificial measure \mathbb{Q} or, by negation, whether x is an outlier relative to the simulations of X . Outlier detection methods have received a lot of attention over decades and, according to Hodge and Austin [6], they generally fall into one of three classes: unsupervised clustering (pinpoints most remote points to be considered as potential outliers), supervised classification (based on both normal and abnormal training data, an observation is classified either as an outlier or not) and semi-supervised detection (based on normal training data, a boundary defining the set of normal observations is formed). We will be using a k NN outlier detection method, which belongs to the first class, and which bases the conclusion of whether x is an outlier or not on the average distance from x to its k nearest neighbors. The motivation for applying this method is two-fold: (i) an extensive empirical study [3] of the unsupervised outlier detection methods concluded that the k NN method, despite its simplicity, is a robust method that remains the state of the art when compared across various datasets, and (ii) given that we already compute the distances to the k nearest neighbors to estimate μ_x , the additional computational burden induced by using the k NN outlier detection method is minimal. For more on outlier detection methods, see [1, 3, 6, 19] and references therein.

Following the setup of Section 2.1, let x_1^s, \dots, x_m^s be realizations of X under \mathbb{Q} and denote by $I_k(x)$ the set of indices corresponding to the k realizations closest to x with respect to some metric d (e.g., the Euclidean or Mahalanobis distance). Then, for observations x_1, \dots, x_n under \mathbb{P} , the algorithm goes as follows:

- (1) For $i = 1, \dots, n$ compute the average distance from x_i to its k -nearest neighbors

$$\bar{d}_i = \frac{1}{k} \sum_{j \in I_k(x_i)} d(x_i, x_j^s).$$

- (2) Obtain a sorted list $\bar{d}_{(1)} \leq \dots \leq \bar{d}_{(n)}$ of $\bar{d}_1, \dots, \bar{d}_n$ and detect, e.g., by visual inspection, a point j at which the structure of the function $i \mapsto \bar{d}_{(i)}$ changes significantly.
- (3) Regard any x_i with $\bar{d}_i \geq \bar{d}_{(j)}$ as an outlier.

Part (ii) of Condition 2.1 can usually not be checked, since we do not have any realizations of Y under \mathbb{P} ; this is similar to the issue of verifying the MAR assumption in an incomplete data problem. Of course, if such realizations are available we can estimate the conditional distribution of Y given $X = x$ under both \mathbb{P} and \mathbb{Q} and compare the results.

3 Application to extreme event estimation for wind turbines

In this section we will consider the possibility of estimating the distribution of the 10-minute maximum down-wind bending moment (load) on the tower top, middle and base on an operating wind turbine from its 10-minute operational statistics. The data consists of 19,976 10-minute statistics from the turbine under normal operation over a period from February 17 to September 30, 2017. Since this particular turbine is part of a measurement campaign, load measurements are available, and these will be used to assess the performance of the surrogate model (see Figure 1 for the histogram and CDF of measured loads).

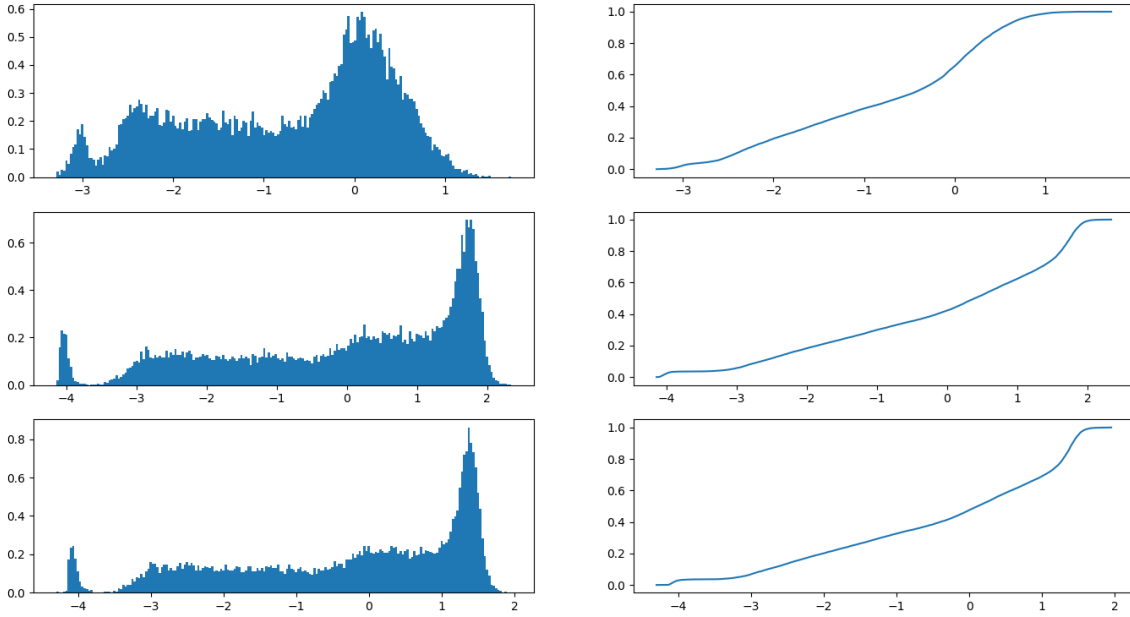


Figure 1: Measured load distributions. Left and right plots correspond to histograms and CDFs, respectively, based on 19,976 observations of the tower top (first row), middle (second row) and base (third row) down-wind bending moments.

To complement the measurements, a simulation tool is used to obtain 50,606 simulations of both the operational statistics and the corresponding tower loads. We choose to use the following eight operational statistics as covariates:

- ▷ Electrical power (maximum and standard deviation)
- ▷ Generator speed (maximum)
- ▷ Tower top down-wind acceleration (standard deviation)
- ▷ Blade flap bending moment (maximum, standard deviation and mean)

▷ Blade pitch angle (minimum)

The selection of covariates is based on a physical interpretation of the problem and by leaving out covariates which from a visual inspection (i.e., plots of the two-dimensional coordinate projections) seem to violate the support assumption imposed in Condition 2.1(i). The loads and each of the covariates are standardized by subtracting the sample mean and dividing by the sample standard deviation (both of these statistics are computed from the simulated values). In the setup of Section 2, this means that we have realizations of $X \in \mathbb{R}^8$ and $Y \in \mathbb{R}$ under both \mathbb{P} and \mathbb{Q} (although the typical case would be that Y is not realized under \mathbb{P}). This gives us the opportunity to compare the results of our surrogate model with the, otherwise unobtainable, estimate (1.1) of $\mathbb{P}(Y \in \cdot)$.

In order to sharpen the estimate of μ_x for covariates x close to the measured ones, we discard simulations which are far from the domain of the measured covariates. Effectively, this is done by reversing the k NN approach explained in Section 2.2 as we compute average distances from simulated covariates to the k nearest measured covariates, sort them and, eventually, choosing a threshold that defines the relevant simulations. We will use $k = 1$ and compute the sorted average distances in terms of the Mahalanobis distance. The selection of threshold is not a trivial task and, as suggested in Section 2.2, the best strategy may be to inspect visually if there is a certain point, at which the structure of the sorted average distances changes significantly. To obtain a slightly less subjective selection rule, we use the following ad hoc rule: the threshold is defined to be $d_{(\tau)}$, the τ -th smallest average distance, where τ is the point that minimizes the L^1 distance

$$d_1(f, f_\tau) := \int_1^m |f(x) - f_\tau(x)| dx \quad (3.1)$$

between the function f that linearly interpolates $(1, d_{(1)}), \dots, (m, d_{(m)})$ and f_τ that linearly interpolates $(1, d_{(1)}), (\tau, d_{(\tau)}), (m, d_{(m)})$ over the interval $[1, m]$ (see the left plot of Figure 2). This selection rule implies a threshold of 6.62 with $\tau = 46, 100$, which in turn implies that 4, 506 (8.90 %) of the simulations are discarded before estimating the conditional load distributions. See the right plot of Figure 2 for a visual illustration of the threshold selection. Of course, a more (or less) conservative selection rule can be obtained by using another distance measure than (3.1).

The same procedure is repeated, now precisely as described in Section 2.2, to detect potential outliers in the measurements. In this case, $k = 10$ is used since this will be the same number of neighbors used to estimate μ_x . The threshold is 2.45 with $\tau = 18, 400$, and hence 1, 577 (8.57 %) of the measurements are found to be potential outliers (see also Figure 3).

To assess which points that have been labeled as potential outliers, two-dimensional projections of the outliers, inliers and simulations are plotted in Figure 4 (if a point seems to be an outlier in the projection plot the original eight-dimensional vector should also be labeled an outlier). To restrict the number of plots we only provide 18

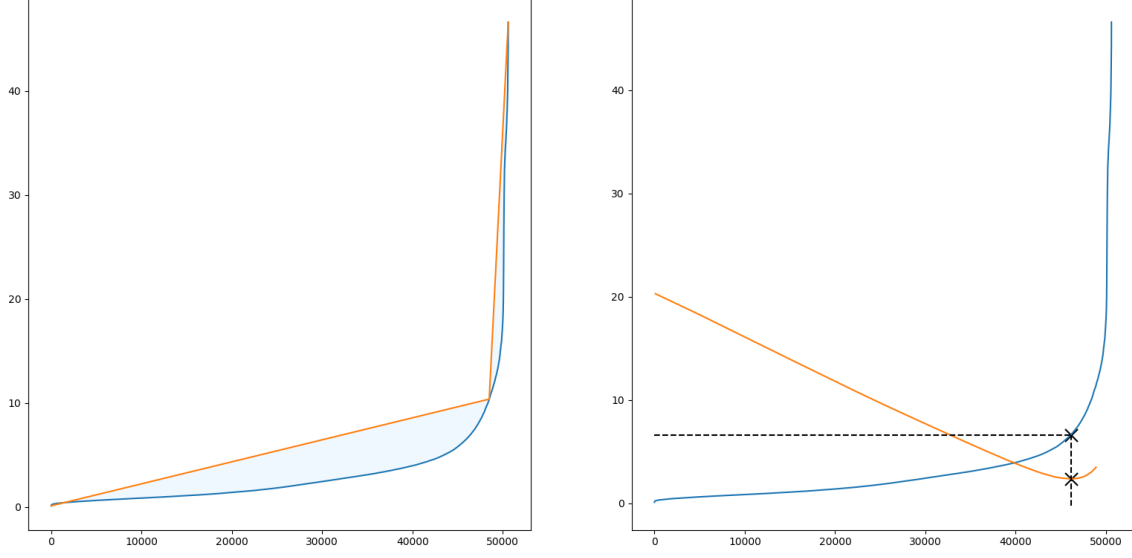


Figure 2: Blue curve: sorted distance from simulated covariates to nearest measured covariates. Left: linear interpolation of $(1, d_{(1)}), (\tau, d_{(\tau)}), (m, d_{(m)})$ with shaded region representing the corresponding L^1 error for $\tau = 48,500$. Right: the orange curve is the normalised L^1 error as a function of τ and the dashed black lines indicate the corresponding minimum and selected threshold.

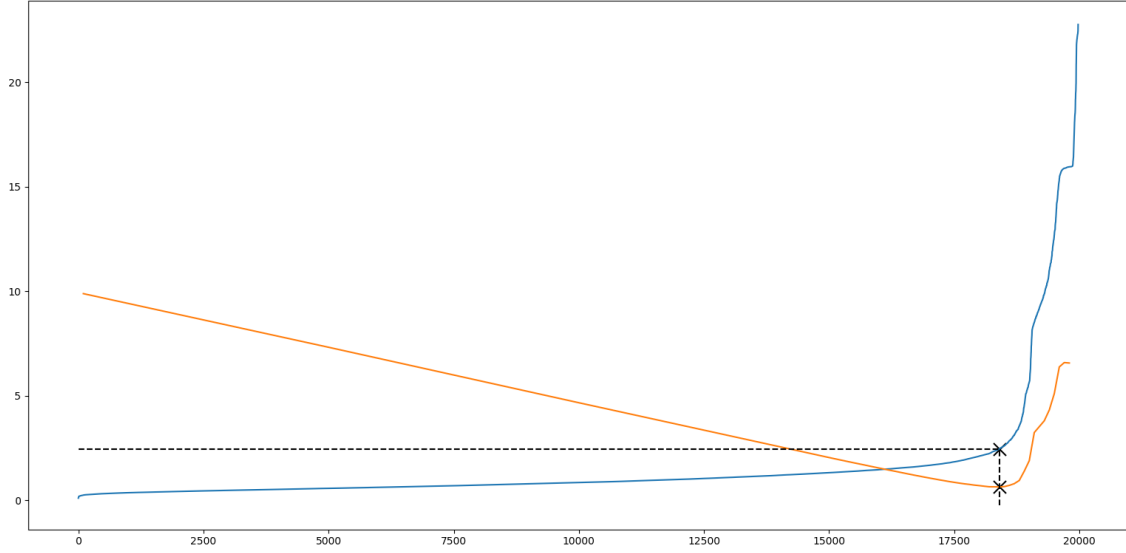


Figure 3: The blue curve is the sorted distance from measured covariates to the 10 nearest simulated covariates, the orange curve is the L^1 error as a function of τ , and the dashed black lines indicate the corresponding minimum and selected threshold. All points with average distance larger than the threshold are labeled possible outliers.

(out of 28) of the projection plots corresponding to plotting electrical power (maximum), blade flap bending moment (maximum) and generator speed (maximum) against each other and all the remaining five covariates. The overall picture of Figure 4 is that a significant part of the observations that seem to be outliers is indeed labeled as such. Moreover, some of the labeled outliers seem to form a horizontal or vertical line, which could indicate a period of time where one of the inputs was measured to be constant. Since this is probably caused by a logging error, such measurements should indeed be declared invalid (outliers).

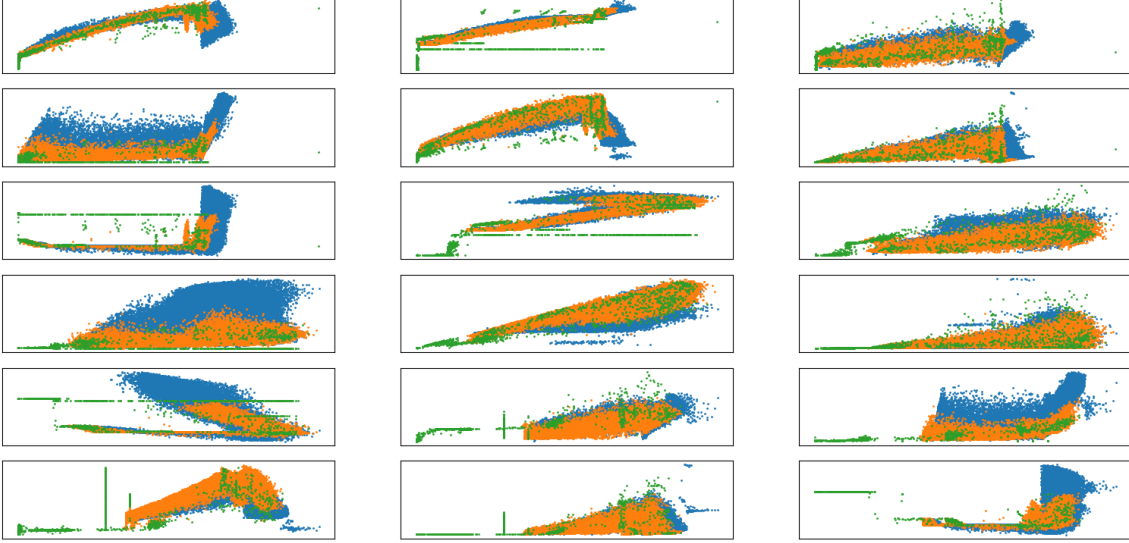


Figure 4: Some of the two-dimensional projections of the covariates. Blue dots are simulations, orange dots are inliers and green dots are potential outliers.

Next, we would need to check if the distributional properties of the load can be expected to change by removing outliers. In an incomplete data setup, the outliers may be treated as the missing observations, and hence we want to assess whether the Missing (Completely) at Random mechanism is in force (recall the discussion in Remark 2.2). If the operation of removing outliers causes a significant change in the load distribution, then the outliers cannot be ignored and would need to be handled separately. In Figure 5 the histograms of tower top, middle and base load obtained from all measurements (the same as those in the three rows of Figure 1) are compared to those where the outliers have been removed. It becomes immediately clear that the distributions are not unchanged, since most of the outliers correspond to the smallest loads of all measurements. However, it seems reasonable to believe that the conditional distribution of the load given that it exceeds a certain (even fairly small) threshold is not seriously affected by the exclusion of outliers. Since the interest is on the estimation of extreme events, i.e., one often focuses only on large loads, it may be sufficient to match these conditional excess distributions. Hence, we choose to exclude the outliers without paying further attention to them. It should

be noted that, since the outlier detection method only focuses on covariates, it does not take into account their explanatory power on the loads. For instance, it might be that a declared outlier only differs from the simulations with respect to covariates that do not significantly help explaining the load level. While this could suggest using other distance measures, this is not a direction that we will pursue here.

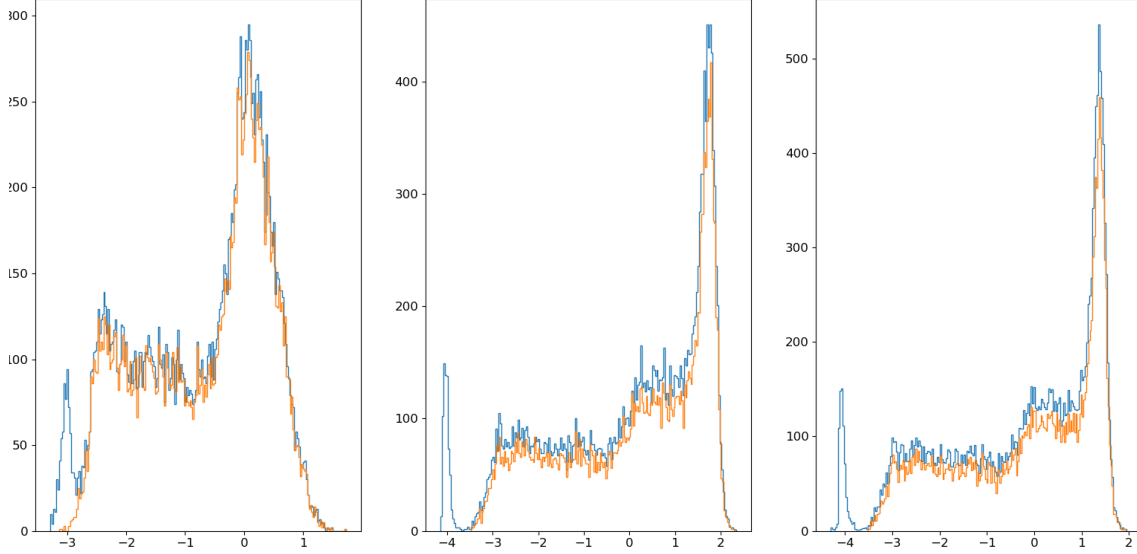


Figure 5: Histograms of measurements on tower top (left), middle (mid) and base (right) downwind bending moments. Measurements including and excluding outliers are represented in blue and orange, respectively.

We will rely on (2.1) together with the two methods presented in Section 2.1 to estimate the load distributions. The unsmoothed version of both methods (i.e., $\sigma = 0$) will be used, and for the k NN method we will choose $k = 10$. There are at least two reasons for initially choosing the bandwidth σ to be zero: (i) it can be a subtle task to select the optimal bandwidth as there is no universally accepted approach, and (ii) given that we have a fairly large dataset, most of the estimated values of the CDFs should be fairly insensitive to the choice of bandwidth. In Figure 6 we have plotted the empirical CDF of the loads (i.e., the CDF of (1.1) based on measured loads) together with the estimates provided by the k NN and random forest approach. Since the loads are 10-minute maxima, it is natural to compare the CDFs to those of GEV type (cf. the Fisher-Tippett-Gnedenko theorem). For this reason, and in order to put attention on the estimation of the tail, we have also plotted the $-\log(-\log(\cdot))$ transform of the CDFs. Recall that, when applying such a transformation to the CDF, the Gumbel, Weibull and Fr chet distributions would produce straight lines, convex curves and concave curves, respectively. From the plots it follows that, generally, the estimated CDFs are closest to the empirical CDF for small and large quantiles. Estimated α -quantiles tend to be smaller than the true ones for moderate values of α . One would expect that, given only the eight

covariates as considered here, a significant part of errors would be due to differences between the simulation environment and the real-world environment. From an extreme event estimation perspective, the most important part of the curve would be the last 10-20 % corresponding to quantiles above 0.8 or 0.9. On this matter, the $-\log(-\log(\cdot))$ transform of the CDFs reveals that the estimated CDFs have some difficulties in replicating the tail of the distribution for middle and base load. However, since there are few extreme observations, this is also the part where a potential smoothing (positive bandwidth) would have an effect. To test the smoothing effect, we choose σ according to Silverman's rule of thumb, that is, $\sigma = 1.06(kn)^{-1/5}\hat{\sigma}_s$, where $n = 18,399$ is the number of measurements (without outliers) and $\hat{\sigma}_s$ is the sample standard deviation of the kn load simulations (top, middle or base) used for obtaining the k NN estimate of the given load distribution. For details about this choice of bandwidth, and bandwidth selection in general, see [16]. In Figure 7 we have compared the $-\log(-\log(\cdot))$ transforms of the smoothed estimates of the CDFs and the empirical CDF.

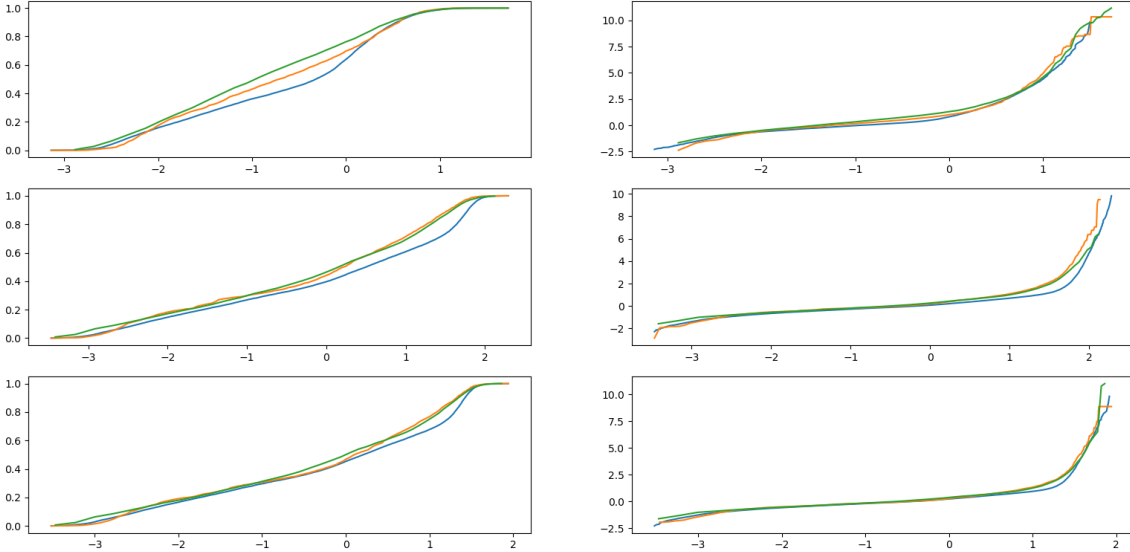


Figure 6: Plots of CDFs (first column) and the corresponding $-\log(-\log(\cdot))$ transforms (second column) of tower top (first row), middle (second row) and base (third row) down-wind bending moments. The blue curve is the empirical distribution of the measurements, and the orange and green curves are the k NN and random forest predictions, respectively.

It seems that the smoothed versions of the estimated curves generally fit the tail better for the tower top and middle loads, but tend overestimate the larger quantiles for the tower base load. This emphasizes that the smoothing should be used with caution; when smoothing the curve, one would need to decide from which point the estimate of the CDF is not reliable (as the Gaussian smoothing always will dominate the picture sufficiently far out in the tail). When no smoothing was used, the uncertainty of the estimates was somewhat reflected in the roughness of

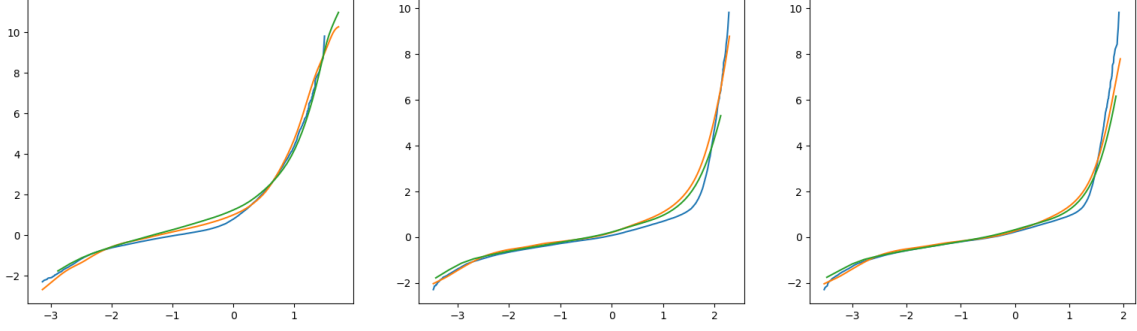


Figure 7: Plots of $-\log(-\log(\cdot))$ transforms of CDFs of tower top (left), middle (center) and base (right) down-wind bending moments. The blue curve is the empirical distribution of the measurements, and the orange and green curves are the smoothed k NN and random forest predictions, respectively, using Silverman’s rule of thumb.

the curves. We end this study with Table 1 which compares some of the estimated quantiles with the true (empirical) ones. From this table we see that the errors tend to be largest for the 25 %, 50 % and 75 % quantiles and fairly small for the 95 %, 99 % and 99.5 % quantiles, which is in line with the conclusion based on Figure 6. Moreover, it also appears that no consistent improvements of the tail estimates are obtained by using the smoothed CDF estimates.

4 Conclusion

In this paper we presented a surrogate model for the purpose of estimating extreme events. The key assumption was the existence of a simulation environment which produces realizations of the vector (X, Y) in such a way that the conditional distribution of the variable of interest Y equals the true one given a suitable set of observable covariates X . It was noted that this corresponds to the Missing at Random assumption in an incomplete data problem. Next, we briefly reviewed the literature on conditional probability estimation as this is the critical step in order to translate valid simulations into an estimate of the true unconditional distribution of Y . Finally, we checked the performance of the surrogate model on real data as we used an appropriate simulation environment to estimate the distribution of the tower top, middle and base down-wind loads on an operating wind turbine from its operational statistics. The surrogate model seemed to succeed in estimating the tail of the load distributions, but it tended to underestimate loads of normal size.

Acknowledgments

We thank James Alexander Nichols from Vestas (Load & Control) and Jan Pedersen for fruitful discussions. This work was supported by the Danish Council for Independent Research (Grant DFF - 4002 - 00003).

Quantile (%)		k NN	k NN (smoothed)	Random forest	Random forest (smoothed)	Empirical
25	Top	-1.7349	-1.7344	-1.7941	-1.7315	-1.5528
	Mid	-1.4252	-1.4434	-1.3607	-1.2773	-1.1427
	Base	-1.4689	-1.4794	-1.4474	-1.3653	-1.3576
50		-0.7111	-0.7106	-0.9544	-0.8928	-0.3204
	—	0.2181	0.2114	0.1587	0.2147	0.5002
		0.1018	0.1152	0.0047	0.0547	0.2087
75		0.1643	0.1626	-0.0501	-0.0055	0.1991
	—	1.1114	1.1076	1.1819	1.2192	1.5460
		0.9407	0.9366	0.9978	1.0247	1.2192
95		0.6936	0.7122	0.6951	0.7414	0.7161
	—	1.6855	1.7090	1.7283	1.7913	1.8670
		1.6782	1.4653	1.4651	1.5184	1.4957
99		0.9611	0.9815	1.0068	1.0631	1.0271
	—	1.8583	1.9383	1.9386	2.0385	1.9917
		1.5877	1.6676	1.6245	1.7240	1.6179
99.5		1.0313	1.0687	1.0944	1.1522	1.1155
	—	1.9180	2.0113	2.0195	2.1213	2.0418
		1.6341	1.7337	1.6716	1.7910	1.6594

Table 1: Some quantiles of the empirical load distributions and of the corresponding k NN and random forest estimates.

References

- [1] Ben-Gal, I. (2005). Outlier detection. In *Data mining and knowledge discovery handbook*, pp. 131–146. Springer.
- [2] Breiman, L. (2001). Random forests. *Machine learning* 45(1), 5–32.
- [3] Campos, G. O., A. Zimek, J. Sander, R. J. Campello, B. Micenková, E. Schubert, I. Assent, and M. E. Houle (2016). On the evaluation of unsupervised outlier detection: measures, datasets, and an empirical study. *Data Mining and Knowledge Discovery* 30(4), 891–927.
- [4] De Haan, L. and A. Ferreira (2007). *Extreme value theory: an introduction*. Springer Science & Business Media.
- [5] Gilli, M. et al. (2006). An application of extreme value theory for measuring financial risk. *Computational Economics* 27(2-3), 207–228.
- [6] Hodge, V. and J. Austin (2004). A survey of outlier detection methodologies. *Artificial intelligence review* 22(2), 85–126.
- [7] Husmeier, D. (2012). *Neural networks for conditional probability estimation: Forecasting beyond point predictions*. Springer Science & Business Media.
- [8] Hyndman, R. J., D. M. Bashtannyk, and G. K. Grunwald (1996). Estimating and visualizing conditional densities. *Journal of Computational and Graphical Statistics* 5(4), 315–336.
- [9] Little, R. J. and D. B. Rubin (2014). *Statistical analysis with missing data*, Volume 333. John Wiley & Sons.
- [10] Neuneier, R., F. Hergert, W. Finnoff, and D. Ormoneit (1994). Estimation of conditional densities: A comparison of neural network approaches. In *ICANN’94*, pp. 689–692. Springer.
- [11] Pedregosa, F., G. Varoquaux, A. Gramfort, V. Michel, B. Thirion, O. Grisel, M. Blondel, P. Prettenhofer, R. Weiss, V. Dubourg, J. Vanderplas, A. Passos, D. Cournapeau, M. Brucher, M. Perrot, and E. Duchesnay (2011). Scikit-learn: Machine learning in Python. *Journal of Machine Learning Research* 12, 2825–2830.
- [12] Ragan, P. and L. Manuel (2008). Statistical extrapolation methods for estimating wind turbine extreme loads. *Journal of Solar Energy Engineering* 130(3), 031011.
- [13] Rosenbaum, P. R. and D. B. Rubin (1983). The central role of the propensity score in observational studies for causal effects. *Biometrika* 70(1), 41–55.

- [14] Rubin, D. B. (1976). Inference and missing data. *Biometrika* 63(3), 581–592.
- [15] Scheffer, J. (2002). Dealing with missing data.
- [16] Silverman, B. W. (2018). *Density estimation for statistics and data analysis*. Routledge.
- [17] Smith, R. L. (1990). Extreme value theory. *Handbook of applicable mathematics* 7, 437–471.
- [18] Sugiyama, M., I. Takeuchi, T. Suzuki, T. Kanamori, H. Hachiya, and D. Okanohara (2010). Least-squares conditional density estimation. *IEICE Transactions on Information and Systems* 93(3), 583–594.
- [19] Zimek, A., E. Schubert, and H.-P. Kriegel (2012). A survey on unsupervised outlier detection in high-dimensional numerical data. *Statistical Analysis and Data Mining: The ASA Data Science Journal* 5(5), 363–387.